Isolation, Catalytic Properties, and Competitive Inhibitors of the Zinc-Dependent Murine Glutaminyl Cyclase†

Stephan Schilling,‡ Holger Cynis,‡ Alex von Bohlen,§ Torsten Hoffmann,‡ Michael Wermann,‡ Ulrich Heiser,‡ Mirko Buchholz,‡ Katrin Zunkel,‡ and Hans-Ulrich Demuth*,‡

Probiodrug AG, Weinbergweg 22, 06120 Halle/Saale, Germany, and ISAS-Institute for Analytical Sciences, Bunsen-Kirchhoff-Strasse 11, 44139 Dortmund, Germany

Received June 14, 2005; Revised Manuscript Received August 11, 2005

ABSTRACT: Murine glutaminyl cyclase (mQC) was identified in the insulinoma cell line β-TC 3 by determination of enzymatic activity and RT-PCR. The cloned cDNA was expressed in the secretory pathway of the methylotrophic yeast *Pichia pastoris* and purified after fermentation using a new three-step protocol. mQC converted a set of various substrates with very similar specificity to human QC, indicating a virtually identical catalytic competence. Furthermore, mQC was competitively inhibited by imidazole derivatives. A screen of thiol reagents revealed cysteamine as a competitive inhibitor of mQC bearing a K_i value of 42 $\pm$2 μM. Substitution of the thiol or the amino group resulted in a drastic loss of inhibitory potency. The pH dependence of catalysis and inhibition support that an uncharged nitrogen of the inhibitors and the substrate is necessary in order to bind to the active site of the enzyme. In contrast to imidazole and cysteamine, the heterocyclic chelators 1,10-phenanthroline, 2,6-dipicolinic acid, and 8-hydroxyquinoline inactivated mQC in a time-dependent manner. In addition, citric acid inactivated the enzyme at pH 5.5. Inhibition by citrate was abolished in the presence of zinc ions. A determination of the metal content by total reflection X-ray fluorescence spectrometry and atomic absorption spectroscopy in mQC revealed stoichiometric amounts of zinc bound to the protein. Metal ion depletion appeared to have no significant effect on protein structure as shown by fluorescence spectroscopy, suggesting a catalytic role of zinc. The results demonstrate that mQC and probably all animal QCs are zinc-dependent catalysts. Apparently, during evolution from an ancestral protease, a switch occurred in the catalytic mechanism which is mainly based on a loss of one metal binding site.

Several bioactive hormones, e.g., thyrotropin-releasing hormone (TRH) or gastrin, possess an N-terminal pyroglutamic acid residue, which is generated from glutamine during prohormone maturation (*1*−*3*). Glutaminyl cyclases (QCs) have been identified to catalyze the cyclization of N-terminal glutaminyl residues in plants and animals (*4*−*6*). However, recent results suggest that these enzymes are also capable of catalyzing the cyclization of N-terminal glutamic acid, liberating a water molecule instead of ammonia (*7*). In the last years, analysis of amyloidotic peptides deposited in familial British dementia, familial Danish dementia, and Alzheimer's disease revealed that these peptides bear pGlu in a considerable amount, likely influencing the degradation and neurotoxicity of these peptides (*8*−*10*). In contrast to the peptide hormones, however, glutamic acid precedes pGlu formation at the N-terminus of these amyloidotic peptides. It was assumed that cyclization of glutamic acid is a spontaneous process (*11*). The specificity of human QC, however, raises the possibility that pGlu-amyloid peptides are generated by enzymatic catalysis (*7*). The first tissue distribution studies of mammalian QCs revealed that they are mainly expressed in brain and some peripheral glands, e.g., thyroid and thymus (*12*, *13*). It is expected that the enzyme is directed to the regulated secretory pathway of the expressing cells where the hormone maturation process takes place (*13*, *14*). Upon stimulation, QCs appear to be secreted from the cells together with the mature hormones (*15*).

QCs from bovine and human sources are the only mammalian enzymes that were isolated so far. The open reading frames of both enzymes consist of 361 amino acids with an overall sequence identity of about 90%. The mature proteins are glycosylated and exhibit a molecular mass of about 40 kDa (*13*, *16*, *17*). Human QC has been shown to be highly specific for the L-configuration of glutamine in the N-terminal amino acid position. Free glutamine was not converted. Other restrictions, however, were not observed, implying that the enzyme is responsible for N-terminal conversion of the very heterogeneous group of pGlu hormones (*18*). Initial mechanistic studies on human QC pointed to an involvement of histidinyl residues in the binding and conversion of the substrate as indicated by diethyl pyrocarbonate inhibition and site-directed mutagenesis (*19*). Later evidence showed that mammalian QCs are structurally related to zinc-dependent aminopeptidases and that the residues for complexation of the active site metal ions are also conserved

† This work was supported by the Federal Ministry of Education and Research of Germany (BMBF), Grant 0313185, to H.-U.D.

* To whom correspondence should be addressed. Tel: 49 345 5559900. Fax: 49 345 5559901. E-mail: Hans-Ulrich.Demuth@probiodrug.de.

‡ Probiodrug AG.

§ ISAS-Institute for Analytical Science.

10.1021/bi051142e CCC: $30.25
Published on Web 09/21/2005

in human QC (*20*, *21*). Furthermore, the metal chelators 1,-10-phenanthroline, dipicolinic acid, and imidazole inhibited human QC, implying a metal-dependent catalysis of the enzyme (*20*). Other potential complexing inhibitors, such as EDTA, peptide thiols, or butaneboronic acid, which inactivate the related aminopeptidases of the clan MH, appeared to be inactive on human QC. In addition, initial attempts to determine the metal content in QC resulted in less than stoichiometric amounts of zinc bound to the enzyme (*21*).

Due to these apparent discrepancies, it was the aim of the present study to isolate mQC[1] in order to gain further insight into general characteristics of the mammalian QCs. Furthermore, the scope of the study focused on the clarification, whether mammalian QCs are metal-dependent catalysts. Answering this question might give a basic picture of the mechanistic background of mammalian QC catalysis.

EXPERIMENTAL PROCEDURES

Materials. The *Escherichia coli* strain DH5α was applied for all plasmid constructions and propagation. *Pichia pastoris* strain X33 (*AOX1*, *AOX2*) was used for the expression of mQC. Yeast was grown, transformed, and analyzed according to the manufacturer's instructions (Invitrogen). Glutaminyl peptides were obtained from Bachem (Bubendorf, Switzerland) or synthesized as described in another study (*18*). Streamline SP XL and butyl-Sepharose 4 Fast Flow were obtained from Pharmacia Biotech (Uppsala, Sweden). Pyroglutamyl aminopeptidase from *Bacillus amyloliqefaciens* was purchased from Qiagen (Hilden, Germany). Imidazole and cysteamine derivatives were from Acros and Sigma. All other materials used were of analytical grade.

Cloning Procedures. The primers for isolation of the open reading frame of mQC were designed using PubMed nucleotide entry AK017598, encoding the putative mQC. The primer sequences were as follows: sense, 5′ ATATGCATGCATGGCAGGCAGCGAAGACAAGC; antisense, 5′-ATATAAGCTTTTACAAGTGAAGATATTCCAACACAAAGAC. Total RNA was isolated from murine insulinoma cell line β-TC 3 cells using the RNeasy mini kit (Qiagen) and reversely transcribed by SuperScriptII (Invitrogen). Subsequently, mQC cDNA was amplified on a 1:12.5 dilution of generated product in a 50 μL reaction with Herculase enhanced DNA polymerase (Stratagene), inserted into the PCR Script CAM cloning vector (Stratagene) and verified by sequencing. The cDNA fragment encoding the mature mQC was amplified using the primers 5′ ATACTCGAGAAAAGAGCCTGGACGCAGGAGAAG (*Xho*I, sense) and 5′ ATATCTAGATTACAAGTGAAGATATTCCAAC (*Xba*I, antisense). The digested fragment was ligated into the vector pPICZαB, propagated in *E. coli* and verified by sequencing of the sense and antisense strand. Finally, the expression plasmid was linearized using *Pme*I, precipitated, and stored at −20 °C.

Transformation of P. pastoris and Miniscale Expression. Plasmid DNA (1−2 μg) was applied for transformation of competent *P. pastoris* cells by electroporation according to the manufacturer's instructions (Bio-Rad). Selection was done on plates containing 100 μg/mL zeocin. To test the recombinant yeast clones upon mQC expression, recombinants were grown for 24 h in 10 mL conical tubes containing 2 mL of BMGY. Afterward, the yeast was centrifuged and resuspended in 2 mL of BMMY containing 0.5% methanol. This concentration was maintained by addition of methanol every 24 h for about 72 h. Subsequently, QC activity in the supernatant was determined. Clones that displayed the highest activity were chosen for further experiments and fermentation.

Large-Scale Expression and Purification. The expression of mQC was performed in a 5 L reactor (Biostad B; B. Braun Biotech, Melsungen, Germany), essentially as described elsewhere (*17*). Briefly, fermentation was carried out in basal salt medium supplemented with trace salts at pH 5.5. Initially, biomass was accumulated in a batch and a fed batch phase with glycerol as the sole carbon source for about 28 h. Expression of mQC was initiated by methanol feeding according to a three-step profile recommended by Invitrogen for an entire fermentation time of approximately 65 h. Subsequently, cells and turbidity were removed from the mQC-containing supernatant by two sequential centrifugation steps at 6000*g* and 38000*g* for 15 min and 4 h, respectively. For purification, the fermentation broth was diluted with water to a conductivity of about 5 mS/cm and applied in reversed flow direction (15 mL/min) onto a Streamline SP XL column (2.5 × 100 cm), equilibrated with 0.05 M phosphate buffer, pH 6.4. After a washing step in reversed flow direction with equilibration buffer for 2 column volumes, proteins were eluted at a flow rate of 8 mL/min using 0.15 M Tris-HCl buffer, pH 7.6, containing 1.5 M NaCl in forward direction. QC-containing fractions were pooled, and ammonium sulfate was added to a final concentration of 1 M. The resulting solution was applied onto a butyl-Sepharose FF column (1.6 × 13 cm) at a flow rate of 4 mL/min. Bound mQC was washed with 0.05 M phosphate buffer, pH 6.8, containing 0.75 M ammonium sulfate for 5 column volumes and eluted in reversed flow direction with 0.05 M phosphate buffer, pH 6.8. The fractions containing mQC were pooled and desalted overnight by dialysis against 0.025 M Tris-HCl, pH 7.5. Afterward, the pH was adjusted to 8.0 by addition of NaOH and applied (4.0 mL/min) onto an Uno Q column (Bio-Rad), equilibrated with 0.02 M Tris-HCl, pH 8.1. After a washing step using equilibration buffer, mQC was eluted using the same buffer containing 0.18 M NaCl. Fractions exhibiting QC activity were pooled, and the pH was adjusted to 7.4 by addition of 1 M Bis-Tris buffer, pH 6.0. mQC was stable at 4 °C for up to 1 month. For long-term storage at −20 °C, 50% glycerol was added.

Enzyme Assays and Analysis. For determination of mQC during the expression and purification, activity was evaluated using H-Gln-βNA at 30 °C, essentially as described (*22*). Briefly, the samples consisted of 0.2 mM fluorogenic substrate, 0.1 unit of pyroglutamyl aminopeptidase in 0.05 M Tris-HCl, pH 8.0, and an appropriately diluted aliquot of QC in a final volume of 250 μL. The excitation/emission wavelength was 320/405 nm. The assay reactions were initiated by addition of QC. One unit is defined as the amount of QC catalyzing the formation of 1.0 μmol of pGlu-βNA from H-Gln-βNA per minute under the described conditions. In the fermentation broth, little interfering aminopeptidatic activity was observed sometimes, depending on the fermen-

[1] Abbreviations: AAS, atomic absorption spectroscopy; GdmCl, guanidinium chloride; ICP-MS, inductively coupled plasma mass spectrometry; H-Gln-AMC, L-glutaminyl-4-methylcoumarinylamide; H-Gln-βNA, L-glutaminyl-2-naphthylamide; mQC, murine glutaminyl cyclase; TXRF, total reflection X-ray fluorescence spectrometry.

tation process. Unspecific cleavage of the QC substrate was determined by omitting the auxiliary enzyme. If necessary, the unspecific cleavage was subtracted from QC activity.

For inhibitor testing, the sample composition was the same as described above, except for the added putative inhibitory compound. Due to the pronounced substrate inhibition by Gln-βNA, inhibitory constants were determined using H-Gln-AMC at a concentration range between 0.25 and 4 K_M. The excitation/emission wavelength was adjusted to 380/460 nm. In contrast to H-Gln-βNA, substrate inhibition by H-Gln-AMC is negligible in the substrate concentration range applied and therefore does not interfere with the kinetic evaluation. The fluorometric assay using H-Gln-AMC was also applied to investigate the pH dependence of the catalytic parameters and inhibitory constants. In these studies, however, the reaction buffer consisted of 0.075 M acetic acid, 0.075 M Mes, and 0.15 M Tris-HCl, adjusted to the desired pH using HCl or NaOH. This buffer provides a constant ionic strength over a very broad pH range (*23*). Evaluation of the acquired enzyme kinetic data was performed using the equations:

$$k_{cat}(\mathrm{pH}) = k_{cat}(\mathrm{limit}) \quad (1)$$

$$K_M(\mathrm{pH}) = K_M(\mathrm{limit})(1 + [H^+]/K_{HS} + K_{E1}/[H^+] + K_{E1}/[H^+]K_{E2}/[H^+]) \quad (2)$$

$$k_{cat}/K_M(\mathrm{pH}) = k_{cat}/K_M(\mathrm{limit})[1/(1 + [H^+]/K_{HS} + K_{E1}/[H^+] + K_{E1}/[H^+]K_{E2}/[H^+])] \quad (3)$$

$$K_i(\mathrm{pH}) = K_i(\mathrm{limit})(1 + [H^+]/K_{HI} + K_{E1}/[H^+] + K_{E1}/[H^+]K_{E2}/[H^+]) \quad (4)$$

in which the left expression denotes the pH-dependent (observed) kinetic parameters. The parameters denoted with limit stand for the pH-independent ("limiting") values. K_{HS}, K_{HI}, K_{E1}, and K_{E2} denote the dissociation constants of the substrate amino group, the basic nitrogen of the imidazole-based inhibitor, and two dissociating groups of the enzyme, respectively. The data of the pH dependencies of the mQC inhibition by cysteamine derivatives were analyzed by assuming one dissociating group. The measurements were performed with a Novostar (BMG Labtechnologies, Germany) or a SpectraFluor Plus (TECAN, Switzerland) reader for microplates.

For investigation of the substrate specificity, mQC activity was studied spectrophotometrically utilizing glutamic dehydrogenase as the auxiliary enzyme (*18*). In contrast to the fluorometric assays, a variety of substrates can be analyzed because of the conversion of ammonia in the coupled reaction. Samples consisted of varying concentrations of the QC substrate (0.25−10 K_M), 0.3 mM NADH, 14 mM α-ketoglutaric acid, and 30 units/mL glutamic dehydrogenase in a final volume of 250 μL. The reaction buffer was 0.05 M Tris-HCl, pH 8.0. Reactions were started by addition of QC and pursued by monitoring of the decrease in absorbance at 340 nm for 8−15 min. The initial velocities were evaluated, and the enzymatic activity was determined from a standard curve of ammonia obtained under assay conditions. All samples were measured at 30 °C, using the Sunrise reader for microplates (TECAN, Switzerland).

Pyroglutamyl aminopeptidase was assayed as described elsewhere (*24*). All kinetic data were evaluated using GraFit software (version 5.0.4 for Windows; Erithacus Software Ltd., Horley, U.K.).

The titrimetric determination of the pK_a values of the amino groups of dimethylcysteamine and cysteamine was carried out at 30 °C using a DL50 Graphix titrator (Mettler-Toledo, Giessen, Germany). Six independent determinations were conducted in order to determine each pK_a value.

mQC Inactivation/Reactivation. Murine QC was inactivated by addition of 2 mM 8-hydroxyquinoline in 50 mM Tris-HCl, pH 8.0 (final mQC concentration 50 μg/mL). Afterward, the sample was dialyzed against four changes [1000-fold excess (v/v), three cycles for 2 h, last cycle overnight] of 0.1 M Bis-Tris, pH 6.8, containing 1 mM EDTA. As controls, native enzyme samples were treated in the same way, except for addition of 8-hydroxyquinoline (control + EDTA) and additionally by omitting 8-hydroxyquinoline and EDTA in the dialysis buffer (control − EDTA). Addition of EDTA was necessary to avoid reactivation of the mQC during dialysis by traces of metal ions present in the buffer.

Reactivation experiments were performed at room temperature using Zn^{2+}, Mn^{2+}, Ni^{2+}, Ca^{2+}, and Co^{2+} ions at final concentrations of 1 mM in 0.1 M Bis-Tris, pH 6.8. A sample of dialyzed QC was added to the respective metal (1/1 v/v) and diluted 10-fold in 0.05 M Tris-HCl, pH 8.0, containing 1 mM EDTA, and the QC activity was determined.

TXRF and AAS Measurements. After purification of mQC as described before, mQC was desalted by size-exclusion chromatography using a Sephadex G-25 fast desalting column (1.0 × 10 cm) which was preequilibrated in 10 mM Tris-HCl, pH 7.6. The QC-containing fractions were collected, the protein was concentrated to 3 mg/mL by ultrafiltration, and the metal content was analyzed. The elution buffer was used as a background control. Element analysis was performed using TXRF. The method offers excellent performance for the simultaneous quantitative determination of the multielement composition (for elements with atomic number $Z \geq 14$) of microsamples (*25*). An Extra II TXRF module containing molybdenum and tungsten primary X-ray sources (Seifert, Ahrensburg, Germany) connected to a Link QX 2000 detector/analyzed device (Oxford Instruments, New Wycombe, U.K.) was used. The X-ray sources were operated at 50 kV and 38 mA. Like all X-ray techniques, TXRF works basically without sample consumption.

Five microliters of undiluted sample solution or control buffer was applied onto the TXRF quartz glass sample support and dried under IR radiation. Afterward, 5 μL of diluted Se aqueous standard solution (internal standard, Aldrich) was added to each sample and dried again. The signals of X-ray fluorescence were allowed to be collected in 100 s. In the case of scarce sample amounts, only a single preparation was analyzed by TXRF in some cases; otherwise, three replicates were used.

With a view toward validation of the results, an independent method was chosen to corroborate the Zn values obtained by TXRF in the samples as well as in the buffer. A state of the art Z-8000 FAAS device (Hitachi, Japan) was used for this purpose. Zn analyses were performed with

Table 1: Purification Scheme of Recombinant Murine QC (mQC) Following Expression in *P. pastoris*

purification step	protein (mg)	QC activity (units)	specific QC activity (units/mg)	yield (%)
fermentation broth	2358	837	0.4	100
cation-exchange chromatography	45	231	5.1	27
hydrophobic interaction chromatography	23.7	156	6.6	19
anion-exchange chromatography	7.5	84	11.2	10

standard parameters using a set of aqueous standard solutions for calibration.

RESULTS

Cloning and Expression of mQC. The murine insulinoma cell line β-TC 3 was identified to express mQC by determination of enzymatic activity and by RT-PCR using primers derived from a putative mQC cDNA which was deposited in the nucleotide database as entry AK017598 (not shown). Subsequently, a cDNA encoding the mature mQC was cloned into pPICZαB. Due to cloning, the signal peptide of murine QC was exchanged by the vector-encoded α-leader of *Saccharomyces cerevisiae* which has been shown to direct heterologous proteins efficiently into the secretory pathway of yeast. *P. pastoris* cells were transformed with the plasmid construct, and the medium was checked on QC activity after growing the cells on methanol. The best expressing clones were subjected to fermentation in a 5 L reactor. For purification, a three-step protocol was established consisting of an initial expanded bed adsorption on a cation-exchange resin, followed by a hydrophobic interaction chromatography and a final anion-exchange chromatography step. The purification process after a typical fermentation is described in Table 1. Usually, 10−20 mg of mQC was isolated after fermentation, corresponding to a yield of about 10%. Fairly homogeneous mQC was obtained after purification, as shown by SDS−PAGE analysis (Figure 1). Protein identity was also characterized by N-terminal sequencing and MALDI-TOF analysis (not shown). Deglycosylation of the protein using endoglycosidase H resulted in a shift of the mQC band in SDS−PAGE corresponding to a mass of about 2 kDa, indicating the mQC is a glycoprotein (not shown).

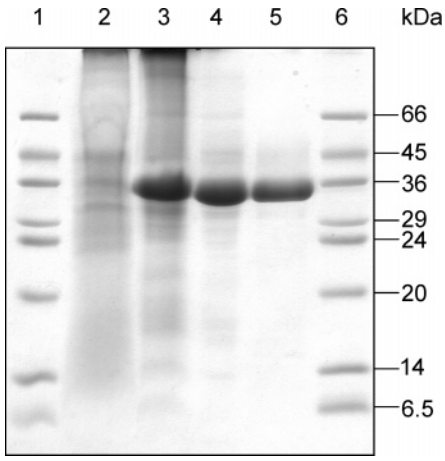

FIGURE 1: SDS−PAGE analysis of the chromatographic steps used to purify murine QC (mQC). Lanes: 1, molecular mass standards (kDa); 2, fermentation broth after centrifugation; 3, the QC-containing fraction after expanded bed adsorption on a cation-exchange resin; 4, purified mQC after hydrophobic interaction chromatography; 5, purified mQC after anion-exchange chromatography; 6, molecular mass standards. Proteins were visualized by Coomassie staining.

Substrate and Inhibitor Specificity. Recently, the substrate specificity of human QC was characterized in detail (*18*). For comparison, the kinetic parameters of conversion of some of these substrates by mQC were also determined (Table 2). The specificity constants for most of the substrates were somewhat lower compared to human QC. These differences are mainly based on higher K_M values; the turnover rates were virtually identical to human QC (*18*, *20*), indicating little differences in substrate binding. As previously observed for human QC (*18*), low specificities were found for dipeptides, especially if they possess small or negatively charged residues in the second amino acid position as, e.g., seen for H-Gln-Gly-OH or H-Gln-Glu-OH. For longer peptides, a slight increase in specificity could be observed. Highest specificities were found for peptides with large hydrophobic residues in the second amino acid position or for dipeptide surrogates.

Imidazole derivatives inhibited the mQC catalysis in a competitive manner (not shown). The K_i values for four inhibitors were analyzed (Table 2). As was previously observed for inhibition of human QC, 1-substituents in-

Table 2: Kinetic Parameters of Substrate Conversion and Inhibition of QC[a]

	murine QC				human QC[b]	
compound	K_M (mM)	k_{cat} (s^{-1})	K_i (mM)	k_{cat}/K_M (mM^{-1} s^{-1})	k_{cat}/K_M (mM^{-1} s^{-1})	K_i (mM)
substrates						
H-Gln-AMC	0.048 ± 0.003	6.0 ± 0.2	5.9 ± 0. 7[d]	125 ± 4	98 ± 2	nd[c]
H-Gln-βNA	0.040 ± 0.004	22 ± 1	1.77 ± 0.18[d]	550 ± 30	294 ± 6	1.21 ± 0.07[d]
H-Gln-Gly-OH	0.41 ± 0.03	12.4 ± 0.2		30 ± 2	53 ± 1	
H-Gln-Ala-OH	0.4 ± 0.02	42 ± 1		105 ± 3	247 ± 4	-
H-Gln-Gln-OH	0.15 ± 0.01	32 ± 1		213 ± 8	140 ± 2	
H-Gln-Glu-OH	0.8 ± 0.06	29 ± 1		36 ± 1	58 ± 1	
H-Gln-Gly-Pro-OH	0.17 ± 0.01	21.6 ± 0.2		127 ± 6	195 ± 7	
H-Gln-Trp-Ala-NH_2	0.072 ± 0.005	41 ± 1		569 ± 26	940 ± 24	
H-Gln-Arg-Gly-Ile-NH_2	0.32 ± 0.02	34 ± 1		106 ± 4	234 ± 4	
H-Gln-Asn-Gly-Ile-NH_2	0.36 ± 0.03	68 ± 2		189 ± 10	329 ± 7	
H-Gln-Thr-Gly-Ile-NH_2	0.16 ± 0.02	23 ± 1		144 ± 12	nd	
inhibitors						
imidazole			0.16 ± 0.01			0.103 ± 0.004
benzimidazole			0.192 ± 0.003			0.138 ± 0.005
methylimidazole			0.023 ± 0.001			0.030 ± 0.001
benzylimidazole			0.0064 ± 0.0007			0.0071 ± 0.0003

[a] Reactions were carried out in 0.05 M Tris-HCl, pH 8.0, at 30 °C. [b] Data from refs *18* and *20*. [c] nd, not determined. [d] Substrate inhibition.

creased the inhibitory potency of imidazole. For the core structures imidazole and benzimidazole, the determined K_i values were slightly higher as compared to human QC. Two 1-substituted imidazole derivatives, methylimidazole and benzylimidazole, however, showed similar inhibitory potency against both enzymes.

The only little differences in selectivity of mQC for various substrates and the imidazole-based competitive inhibitors compared to human QC reflect the high degree of sequential and hence structural conservation of mammalian QCs.

Inhibition by Chelators. The inhibition of porcine QC by the heterocyclic chelator 1,10-phenanthroline was reported already in one of the first studies on QC (*1*). Recently, we performed an extended study on the inhibitory specificity of human QC (*20*). Besides 1,10-phenanthroline, also dipicolinic acid inhibited the QC catalysis in a time-dependent manner. EDTA, however, did not inactivate the enzyme even at concentrations above 20 mM. These findings were also corroborated with mQC (not shown). Additionally, we tested another heterocyclic chelator, 8-hydroxyquinoline, as inhibitor of mQC catalysis. As was observed for the other inhibitory active heterocyclics, addition of 8-hydroxyquinoline to the QC assay resulted in time-dependent inhibition of substrate conversion (Figure 2A). Due to treatment of the enzyme with the chelator, it was possible to isolate inactive mQC after dialysis against buffer containing 1.0 mM EDTA. The isolated enzyme could be fully reactivated by addition of $ZnSO_4$. Significant reactivation was also observed with cobalt and nickel ions (Figure 2B). Addition of EDTA during dialysis was necessary in order to avoid a reactivation of the enzyme by transition metals present in the buffer solutions. EDTA had no influence on QC activity during dialysis (Figure 2B).

Inactivation of mQC was also observed by incubation in citrate buffer at pH 5.5 (Figure 2C). In contrast, at neutral pH, mQC activity was fairly stable during the time of incubation. Furthermore, inactivation by citric acid could be prevented by addition of $ZnSO_4$, indicating an inhibition due to release of zinc from mQC.

Inhibition by Cysteamine Derivatives. The only potent competitive inhibitors of QC known thus far base on an imidazole or imidazole-related core structure. The putatively related bacterial aminopeptidases are inhibited competitively by peptide thiols (*26*). An inhibition of human QC by one of these compounds, however, could not be detected (*20*). In contrast, a screening run of several thiols available revealed a potent competitive inhibition of mQC by cysteamine, exhibiting a K_i value of 42 ± 2 μM. The plot of the slopes obtained from the Lineweaver−Burk evaluation was strictly linear, effectively ruling out mixed-type inhibition (Figure 3). An initial investigation of structurally related compounds revealed a necessity of both amino and thiol group for potent inhibition (Table 3). Modification of the thiol group resulted in a drastic drop of inhibitory potency as shown for ethylenediamine and ethanolamine. In addition, the amino group of cysteamine plays a crucial role for inhibitor binding. However, its modification did not lead to a complete loss of inhibition, as indicated by mercaptoethanol or ethylmercaptan.

Interestingly, N-alkylation appears to be beneficial for binding as revealed by the potent inhibition of mQC by dimethyl- and diethylcysteamine (Table 3).

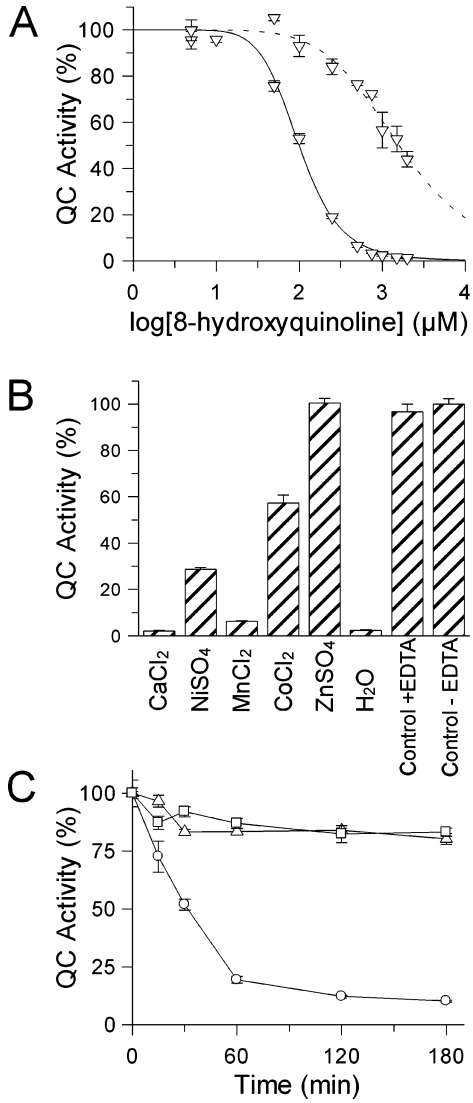

FIGURE 2: Influence of chelating agents and metal ions on mQC activity. (A) Time-dependent inhibition of mQC by 8-hydroxyquinoline. mQC activity was determined at 30 °C using H-Gln-AMC in 0.05 M Tris-HCl, pH 8.0. Varying concentrations of the chelator were added to mQC, and activity was determined immediately (dotted trace) or after 15 min of incubation (continuous trace). (B) Reactivation of mQC with divalent metals. Prior to reactivation, mQC was inactivated to a residual activity of 1−2% by addition of 1 mM 8-hydroxyquinoline in 0.05 M sodium phosphate, pH 7.5. Subsequently, the enzyme was subjected to dialysis against 0.05 M Bis-Tris, pH 6.8, containing 1 mM EDTA. Reactivation of mQC was investigated by addition of a 2 mM stock solution of different metal ions to the inactivated enzyme (dilution, 1:2 v/v). Controls are given by enzyme samples that were not inactivated but also dialyzed against EDTA solution as the inactivated enzyme (+EDTA) and by enzyme samples that were dialyzed against buffer solutions without adding EDTA (−EDTA). (C) Inactivation of mQC by citric acid. mQC was incubated in 0.15 M sodium citrate buffer at pH 5.5 (circles). At the indicated times, enzyme samples were removed, and the QC activity was determined using H-Gln-AMC in 0.05 M Tris-HCl, pH 8.0, containing 1.0 mM EDTA. EDTA was added to the reaction buffer in order to avoid a rapid reactivation of mQC by traces of zinc present in buffer solutions. Inactivation of mQC by citrate could be halted by addition of 100 μM $ZnSO_4$ during incubation (squares). Also, incubation of mQC in 0.05 M Bis-Tris, pH 6.8, for the same time did not result in significant inactivation (triangles).

pH Dependence of Catalysis and Inhibition. On the basis of the continuous coupled QC assays we described previously (*22*), the first detailed pH dependence study for conversion

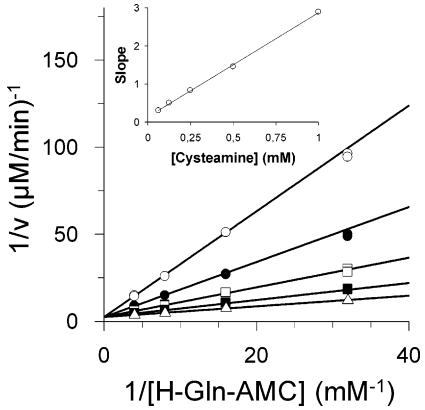

FIGURE 3: Lineweaver−Burk plot for mQC-catalyzed cyclization of H-Gln-AMC in the presence of various concentrations of cysteamine between 0.0625 and 1.0 mM. The inset shows a plot of the determined slope versus the inhibitor concentrations. The reactions were carried out in 0.05 M Tris-HCl, pH 8.0, at 30 °C.

Table 3: Inhibition of mQC by Cysteamine Derivatives and Derived Compounds[a,b]

Compound	K_i-value (µM)	Structure
cysteamine	42 ±2	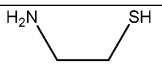
N-dimethylcysteamine	29 ±2	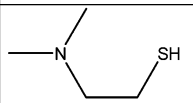
N-diethylcysteamine	10.9 ±0.3	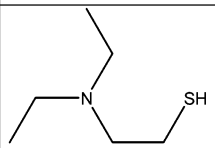
mercaptoethanol	2580 ±160	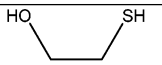
ethylmercaptane	n.d.[c]	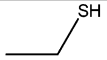
ethylenediamine	22000 ±1500	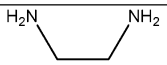
ethanolamine	19300 ±1100	
ethylamine	n.i.	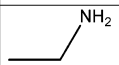

[a] Reactions were carried out in 0.05 M Tris-HCl, pH 8.0, at 30 °C. [b] ni, no inhibition detected at [S] = K_M and [I] = 10 mM; nd, not determined. [c] 60% residual mQC activity at [S] = $4K_M$ and [I] = 10 mM.

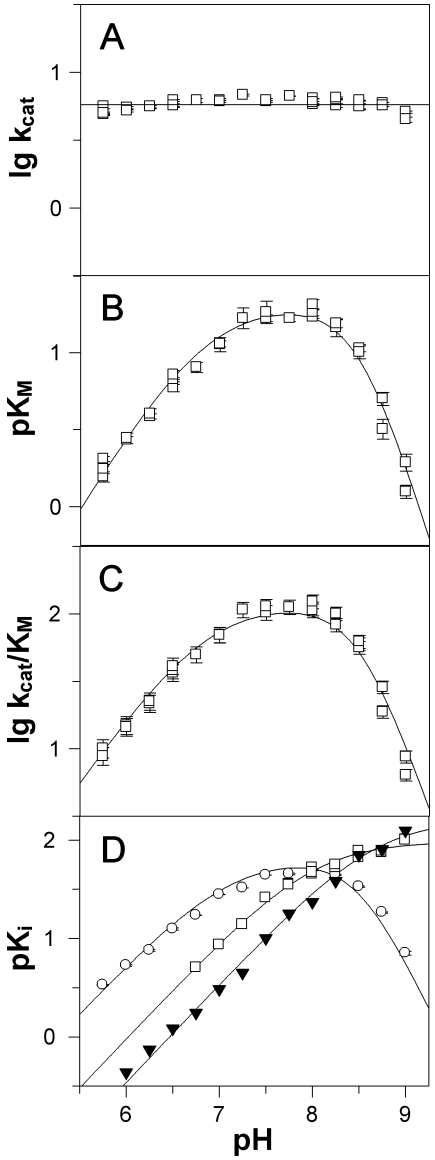

FIGURE 4: pH dependence of the kinetic parameters for the mQC-catalyzed cyclization of H-Gln-AMC and for the inhibition of this cyclization by three competitive inhibitors. (A) pH dependence of k_{cat}. Data points are well described by the assumption of pH independence. (B) pH dependence of K_M. The theoretical curve was calculated using eq 2, with $pK_{HS} = 6.83$, $pK_{E1} = 8.9$, $pK_{E2} = 8.1$, and $K_M(\text{limit}) = 0.047$ mM. (C) pH dependence of k_{cat}/K_M. The theoretical curve was calculated using eq 3 with the same values used for the constants as in the theoretical curve of (B) and $k_{cat}/K_M(\text{limit}) = 123\ \text{mM}^{-1}\ \text{s}^{-1}$. (D) pH dependence of K_i for the inhibitors 1-methylimidazole (circles), cysteamine (triangles), and *N*,*N*-dimethylcysteamine (squares). The theoretical curve for 1-methylimidazole was calculated using eq 4, with $pK_{HI} = 7.05$, $pK_{E1} = 8.9$, $pK_{E2} = 8.1$, and $K_i(\text{limit}) = 0.015$ mM. The pH dependencies of inhibition by the cysteamine derivatives were fitted according to single dissociation curves. Fitting results were $pK_a = 8.7 \pm 0.1$ and $K_i(\text{limit}) = 0.006 \pm 0.001$ mM for cysteamine and $pK_a = 8.00 \pm 0.03$ and $K_i(\text{limit}) = 0.0104 \pm 0.0004$ mM for *N*,*N*-dimethylcysteamine.

of H-Gln-AMC by a mammalian QC was performed using mQC (Figure 4A−C). Prior to analysis, we examined the pH-dependent stability of mQC and the auxiliary enzyme pyroglutamyl aminopeptidase. Both enzymes were stable in the pH range between 5.5 and 9.0 for 30 min at 30 °C (not shown). At pH values below or above, mQC was inactivated rapidly. By addition of 20 μM $ZnSO_4$, denaturation in the acidic range could be partially prevented. However, we detected an inhibition of the auxiliary enzyme by trace amounts of zinc. Therefore, the range of analysis was limited to pH 5.5−9.0.

As shown in Figure 4A, the turnover number of mQC was virtually unchanged in the pH range of analysis. A slight decrease of k_{cat} was observed in the basic region, which might imply a decrease of k_{cat} due to deprotonation of an essential group of the enzyme or a change in the rate-determining

step of catalysis. However, the small number of data points collected in this pH range prevented a reliable determination of the corresponding putative dissociation constant. Because of the independence of k_{cat} on pH, the shapes of the curves of the kinetic parameters K_M and k_{cat}/K_M are characterized by the same dissociation constants in the pH range between 5.5 and 9.0 (Figure 4B,C). In the acidic range, the slopes of both curves indicate dependence of substrate binding on the unprotonated substrate H-Gln-AMC as suggested by the dissociation constant of 6.85, which is in good agreement with the pK_a of the substrate amino group [6.83 ±0.01 (*20*)]. In the basic range above pH >8.25, K_M increases (Figure 4B). The inflections of the curve can be interpreted by deprotonation of two dissociating groups of the enzyme possessing pK_a values of 8.1 and 8.9.

Interestingly, the pH dependence of inhibition by cysteamine, dimethylcysteamine, and 1-methylimidazole showed conspicuous differences (Figure 4D). While the pH dependencies in the acidic range for all inhibitors tested show one inflection of a corresponding pK_a value that is close to the respective pK_a of the unprotonated nitrogen, only 1-methylimidazole causes a pH-dependent increase of the K_i value in the basic pH region. Apparently, imidazole derivatives interact with the active site of mQC in a different manner than cysteamine and its derivatives.

Determination of the Metal Content of mQC. The time dependency of the inactivation of mQC by different chelators and the efficient reactivation of the apoenzyme by zinc ions suggest the necessity of bound zinc for the catalysis of the enzyme. The stoichiometry of zinc binding by QC, however, is not addressed by these experiments. Therefore, we used mQC purified from several fermentations and analyzed the enzyme samples using TXRF. This method offers the chance to analyze complex mixtures in parallel, requiring only minute quantities of sample.

Several elements were detected in the enzyme samples. Some of these are originally contained in the buffer used, e.g., Cl, K, Ca, Fe, and Br. They do not differ significantly in their concentrations in the controls as well as in the enzyme samples. In addition to these elements, some traces of the elements Ni and Cu and appreciable amounts of S and Zn could be detected in mQC-containing samples (Figure 5). In contrast, the elution buffer control did not display a zinc signal at all. Quantification of the zinc content of three independent enzyme samples resulted in a zinc content of 0.94 ± 0.09 mol of zinc/mol of enzyme. This result was entirely corroborated by the parallel determination of the samples using AAS, yielding 0.9 ± 0.1 mol of zinc/mol of mQC (not shown).

Influence of Zinc Release on the Protein Structure. To investigate the influence of zinc release on the structure of mQC, fluorescence spectra of the enzyme were recorded. In the presence of 300 μM heterocyclic chelator 2,6-dipicolinic acid, mQC was inactivated to a residual activity of 3% at pH 7.2 (Figure 6A). The same experimental conditions were applied for an investigation of putative structural changes caused by the release of the metal ion by dipicolinic acid. During the time of inactivation, fluorescence emission spectra were recorded after excitation at 295 nm (Figure 6B). Interestingly, mQC inactivation appears to be accompanied only by little structural changes, as indicated by a slight decrease in fluorescence intensity after 2 h of incubation.

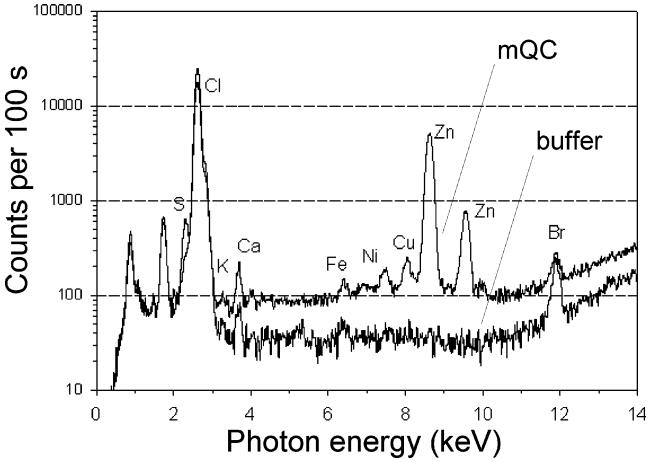

FIGURE 5: Superposition of total reflection X-ray fluorescence (TXRF) spectra of a mQC preparation and of elution buffer. mQC was purified as shown in Figure 1 and desalted by size-exclusion chromatography. The elution buffer (10 mM Tris-HCl, pH 7.6) is shown as a background control. The evaluation of the measurements reveals equimolar amounts of zinc bound to the enzyme.

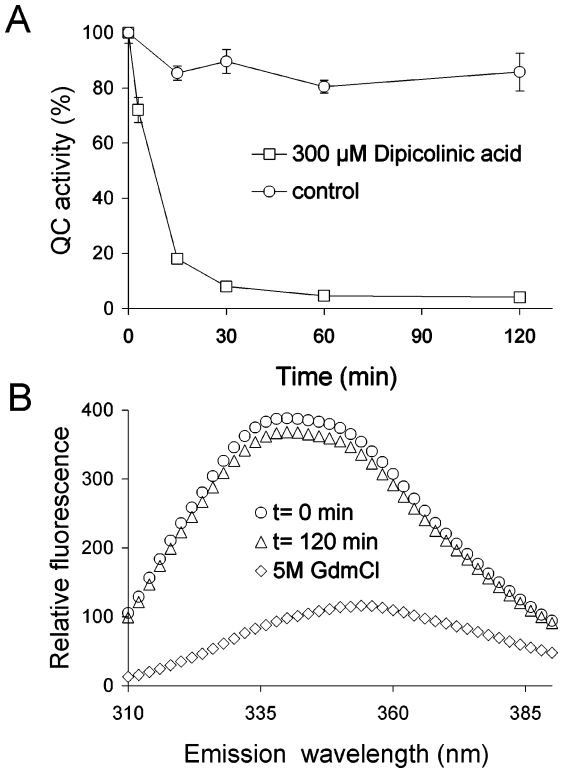

FIGURE 6: Influence of zinc depletion on mQC structure. (A) mQC was inactivated using 300 μM dipicolinic acid in 50 mM Mops buffer and 300 mM NaCl, pH 7.2 (squares). At the times indicated, residual activity was determined using H-Gln-βNA in 50 mM Tris-HCl, pH 8.0, containing 1 mM EDTA under standard conditions. Residual activity dropped to 3% after 2 h of incubation. mQC was stable in the absence of the chelating agent (circles). (B) Fluorescence emission spectra of mQC (0.2 μM) after excitation at 295 nm. The protein was dissolved in 50 mM Mops buffer, 300 mM NaCl, and 300 μM dipicolinic acid, pH 7.2, and spectra were recorded directly after addition of the chelating agent (circles, t = 0 min) and after 2 h of incubation (triangles, t = 120 min). A spectrum of unfolded mQC was obtained in 50 mM Mops, pH 7.2, containing 5 M GdmCl (squares).

Furthermore, the fluorescence emission maximum remained unchanged at 340 nm, indicating that the environment of the tryptophanyl residues did not change significantly upon

```
Murine QC   MAGSEDKRVVGTLHLLLLQATVLSLTAGNLSLVSAAWTQEKNHHQPAHLNSSSLQQVAEG
Human QC    MAGGRHRRVVGTLHLLLLVA-ALPWASRGVSPSASAWPEEKNYHQPAILNSSALRQIAEG
Bovine QC   MAGCRDPRVVDTLHLLLLVA-VLPLAVSGVRRGAVDWTQEKNYHQPALLNVSSLRQVAEG
            *** .. ***.******* * .*. :  .:   :  *.:***:**** ** *:*:*:***

SGAP        ------------------AP-DIPLA----------------------------NVKAHL
                             .  :. :                               .  *.

Murine QC   TSISEMWQNDLRPLLIERYPGSPGSYSARQHIMQRIQRLQAEWVVEVDTFLSRTPYGYRS
Human QC    TSISEMWQNDLQPLLIERYPGSPGSYAARQHIMQRIQRLQADWVLEIDTFLSQTPYGYRS
Bovine QC   TSISEMWQNDLRPLLIERYPGSPGSFAARQHIMQRIQRLQADWVLEVDTFLSQTPYGYRS
            ***********:*************::**************:**:*:*****:*******

SGAP        TQLSTIAANNGG----NRAHGRPGYKASVDYVKAKLD--AAGYTTTLQQFTSGGATGYNL
            *.:* :  *:      :*  * **  :: :::  :::   * :.  :: * *  . **.

Murine QC   FSNIISTLNPEAKRHLVLACHYDSKYFPRWDSRVFVGATDSAVPCAMMLELARALDKKLH
Human QC    FSNIISTLNPTAKRHLVLACHYDSKYFSHWNNRVFVGATDSAVPCAMMLELARALDKKLL
Bovine QC   FSNIISTLNPTAKRHLVLACHYDSKYFPHWDDRVFVGATDSAVPCAMMLELARALDKQLF
            ********** ****************.:*:.************************:*

SGAP        IAN---WPGGDPNKVLMAGAHLDSV-------SSGAGINDNGSGSAAVLETALAVSR---
            ::*     .  .:: *: ..* **           .* .*..  .* :** * *:.:

Murine QC   SLKDVSGSKPDLSLQLIFFDGEEAFHHWSPQDSLYGSRHLAQKMASSPHPPGSRGTNQLD
Human QC    SLKTVSDSKPDLSLQLIFFDGEEAFLHWSPQDSLYGSRHLAAKMASTPHPPGARGTSQLH
Bovine QC   SLKNISDSRPDLSLQLIFFDGEEAFHLWSPQDSLYGSRHLASKMASTPHPPGARDTNQLH
            *** :*.*:****************  ************** ****:*****:*.*.**.

SGAP        -----AGYQPDKHLRFAWWGAEEL--------GLIGSKFYVNNLPSADRSKLAGYLN---
                 :. :**  *:: ::..**          .* **:. . ::.*: :.  :   .

Murine QC   GMDLLVLLDLIGAANPTFPNFFPKTTRWFNRLQAIEKELYELGLLKDHSLERKYFQNFGY
Human QC    GMDLLVLLDLIGAPNPTFPNFFPNSARWFERLQAIEHELHELGLLKDHSLEGRYFQNYSY
Bovine QC   GMDLLVLLDLIGAPFPTFPNFFPNTARWFGRLEAIEHGLRELGLLKDHSSERWYFRNYGY
            ************. ********:::*** **:***: * ********* *  **:*:.*

SGAP        -------FDMIGSPNPGY--FVYDDDPVIEK--TFKNYFAGLNVPTEIETE---------
                   :*:**:. * :  *. .    : :  :::: :  *.: .: . *

Murine QC   GNIIQDDHIPFLRKGVPVLHLIASP-------------------FPEVWHTMDDNEENLH
Human QC    GGVIQDDHIPFLRRGVPVLHLIPSP-------------------FPEVWHTMDDNEENLD
Bovine QC   GGVIQDDHIPFLRRGVPVLHLISSP-------------------FPEVWHTMDDNEENLD
            *.:**********:********.**                    ***************.

SGAP        -GDGRSDHAPFKNVGVPVGGLFTGAGYTKSAAQAQKWGGTAGQAFDRCYHSSCDSLSNIN
             .  :.** ** . ****  *:...                    * . :*:  *. .*:.


Murine QC   ASTIDNLNKIIQVFVLEYLHL-------
Human QC    ESTIDNLNKILQVFVLEYLHL-------
Bovine QC   RTTIDNLNKILQVFVLEYLHL-------
            :********:**********

SGAP        DTALDR-NSDAAAHAIWTLSSGTGEPPT
             :::*. *.   ...:  *
```

FIGURE 7: Sequence alignment of the primary structures of QCs from a bovine (361 amino acids), human (361 amino acids), and murine (362 amino acids) origin. Sequence identity is about 80% between all proteins. Differences are mainly evident in the N-terminal signal sequences that direct the proteins to the secretory pathway. In contrast to human and bovine QC, which contain two N-glycosylation sites located at asparagines 49 and 296 or 183, respectively, murine QC has only one such site (asparagine 50). Sequence alignment was extended by the aminopeptidase of *S. griseus*, a family type member of the aminopeptidase family M28A, in which QCs are deposited in the MEROPS database. The residues of zinc complexation (bold) are conserved in all mammalian QCs.

inactivation of mQC. The impact of unfolding of mQC is illustrated by the emission spectrum obtained in 5 M GdmCl (Figure 6B). Upon unfolding, the fluorescence intensity drops drastically and is accompanied by a change in the fluorescence emission maximum to 355 nm, which is characteristic for tryptophan in aqueous solution.

DISCUSSION

Our recent studies were focused on comparison of the QCs from plants and mammals and revealed that the proteins from these origins show similarities neither in terms of structure nor in inhibitory specificity (*18*, *20*, *27*). In contrast, mammalian QCs display a high homology of their primary structure, as revealed by a sequence alignment of the human, murine, and bovine QC, the proteins that were cloned until now (Figure 7). As shown in the present study, this conservation in sequence is well reflected by the almost identical substrate and inhibitory specificity of mQC and human QC (Table 2). The specificity constants for conversion of each substrate differed by far less than 2-fold between human and murine QC. Similarity between both proteins is even more evident in the case of the K_i values of imidazole-based inhibitors, suggesting virtually identical modes of inhibitor binding and substrate conversion.

On the basis of the inhibitory specificity and the similarity of the primary structure to bacterial aminopeptidases of the

clan MH, a zinc-dependent catalysis was proposed previously for human QC (*20*). Some debate, however, was raised after the determination of the zinc content of human QC by ICP-MS (*21*). Additionally, the authors based their conclusion of a metal-independent mechanism of mammalian QCs on the finding that EDTA and peptide thiols, chelators that inhibit the related aminopeptidases of the clan MH, do not inhibit QC (*20*, *26*). In fact, we also could not detect an inhibition of mQC by EDTA. However, there are several examples known of zinc-dependent aminopeptidases that are not susceptible to inactivation by EDTA but which are sensitive to heterocyclic chelators (*28*, *29*). Moreover, as shown in Figure 7, the zinc-binding motif of the aminopeptidase of *Streptomyces griseus*, the prototype peptidase of family M28B of the metalloaminopeptidases, in which QC is deposited in the MEROPS database (www.merops.sanger.uk), is conserved in all mammalian QCs that were cloned to date. Finally, the inactivation of mQC by the chelators 1,10-phenanthroline, 2,6-dipicolinic acid, 8-hydroxyquinoline, and citrate, the potent reactivation by zinc ions, and the stoichiometric amounts of zinc found in mQC using TXRF and AAS clearly suggest mQC being a metalloenzyme (Figures 2 and 4).

In addition to clarifying the metal dependence of QC, our efforts to further characterize the inhibitory specificity of mammalian QCs resulted in the identification of cysteamine and cysteamine derivatives as a second class of potent competitive inhibitors (Figure 3 and Table 3). Substitution of either functional group of the compounds results in a drop of inhibitory potency (Table 3), indicating a specific binding of the inhibitors to the active site of mQC mediated by interactions of both groups. Interestingly, inhibition by cysteamine depends strongly on presence of both the thiol and the amino group. However, the thiol group appears more important for binding, since modification results in a more drastic decrease in inhibitory potency as exemplified by aminoethanol, ethylenediamine, and ethylamine. Substitution of the amino group yielded inhibitory compounds with only about 100-fold reduced potency, e.g., mercaptoethanol and ethylmercaptan. Thus, apparently the thiol of the inhibitors provides a dominating contribution to binding. In contrast to cysteamine, however, the inhibitory potency of imidazole was thought to depend only on the interaction of the basic nitrogen with the active site of QC (*20*).

Differences of the binding mode between cysteamine derivatives and imidazoles become also evident comparing the pH dependence of QC inhibition by cysteamine, dimethylcysteamine, and 1-methylimidazole (Figure 4). While the K_i values in the case of the cysteamine derivatives appear to depend only on the protonation status of the inhibitor, the K_i value of 1-methylimidazole is also influenced by the protonation status of the mQC active site, similar to that seen by the pH dependencies of the substrate H-Gln-AMC and the inhibitor 1-methylimidazole in the basic pH region (Figure 4B,D). Obviously, deprotonation of two dissociating groups of the enzyme leads to diminished binding of the substrate and the imidazole-based inhibitor. Reduction in affinity might be caused by deprotonation and subsequent alterations in the active site structure leading to disruption of a binding site, e.g., the hydrophobic interaction to the imidazole ring and the hydrophobic AMC residue of the substrate. Similar results were obtained with butaneboronic acid and one of the related aminopeptidases (*30*). In contrast to 1-methylimidazole, no drop of inhibitory potency was observed with the cysteamine derivatives in the basic pH region (Figure 4D), demonstrating differences in the binding mode of the competitive inhibitors. Besides these differences, the pH dependencies for the binding of the inhibitors and the substrates also show similarities. All require an unprotonated nitrogen for binding to the active site; i.e., they must be free of positive charge, as indicated by the acidic shapes of the pH dependencies.

In light of the proven zinc content of mQC and the results of the investigations regarding the pH dependence and structural requirements for inhibition, it is tempting to speculate that, in the case of the cysteamine-derived inhibitors, the thiol and, in the case of the imidazole derivatives, a ring nitrogen interact with the active site zinc ion. Probably, binding of the amino group of cysteamine accords then to the binding mode of the substrate amino group. This, in turn, would implicate that the γ-carbonyl of the substrate glutaminyl residue interacts with the active site zinc, which enforces the polarity of the carbonyl and accelerates the nucleophilic attack of the amino group, as suggested previously for human QC (*20*).

A catalytic role of zinc is further implicated by the structural integrity of mQC after removal of the zinc ion, demonstrating that zinc is not required for stabilizing the overall structure of the protein (Figure 6). Furthermore, this is suggested by the homology to the aminopeptidases that require zinc for their catalytic activity. The peptidases of the clan MH, however, contain two zinc ions in the active site in order to exert their catalytic function. Thus, apparently during evolution of QC from an ancestral protease there was a possible switch of the catalytic mechanism that is mainly based on disruption of one zinc binding site. It is still unclear, however, which residues ligate the zinc ion in the active site. As shown in Figure 7, apparently all five residues coordinating the two zinc ions in the aminopeptidase of *S. griseus* (SgAP) are also found in mammalian QCs. Initial studies using site-directed mutagenesis point to a crucial role of the two histidines and glutamic acid residues, which are responsible for zinc binding in clan MH proteins, for catalytic activity of human QC (*19*, *21*). In contrast, mutagenesis of the two aspartic acid residues was reported to have no effect on catalysis (*21*). Thus, in mammalian QCs possibly one of the glutamic acid residues and the two histidines are responsible for zinc complexation. Although these results are still the subject of further studies, the present results suggest a substantial change in zinc-complexation geometry during evolution of these enzymes. Final clarification might only be achieved by the solution of the protein crystal structure.

In conclusion, our results obtained with the newly cloned and analyzed murine QC support that all mammalian QCs are zinc-dependent catalysts. Obviously, the QCs evolved from aminopeptidases by a reorganization of the active site, accompanied by a loss of one zinc ion binding site. Further analysis of the catalytic mechanism and the zinc ion binding mode in QCs will give interesting insights into the evolutionary mechanisms that were required to provoke a change from an zinc-dependent hydrolase into a zinc-dependent transferase.

ACKNOWLEDGMENT

We thank Dr. J.-U. Rahfeld and J. Eggert for critical reading of the manuscript.

NOTE ADDED IN PROOF

During final processing of this paper, Huang et al. (*31*) published the 3D structure of human QC. The work reveals hQC as a zinc-dependent enzyme proving previous results obtained with hQC (*20*) and strongly backing our conclusion of the current article that all mammalian QCs are stoichiometric metal binding catalysts. Moreover, the work also supports our discovery (*7*) of plant and mammalian QCs as catalysts of glutamate cyclization and inhibition as a potential new therapeutic approach to treating pyroglutamate-peptide mediated amyloidosis.

REFERENCES

1. Busby, W. H. J., Quackenbush, G. E., Humm, J., Youngblood, W. W., and Kizer, J. S. (1987) An enzyme(s) that converts glutaminyl-peptides into pyroglutamyl-peptides. Presence in pituitary, brain, adrenal medulla, and lymphocytes, *J. Biol. Chem. 262*, 8532−8536.
2. Garavelli, J. S. (2000) The RESID database of protein structure modifications: 2000 update, *Nucleic Acids Res. 28*, 209−211.
3. Goren, H. J., Bauce, L. G., and Vale, W. (1977) Forces and structural limitations of binding of thyrotrophin-releasing factor to the thyrotrophin-releasing receptor: the pyroglutamic acid moiety, *Mol. Pharmacol. 13*, 606−614.
4. Messer, M. (1963) Enzymatic cyclization of L-glutamine and L-glutaminyl peptides, *Nature 4874*, 1299.
5. Messer, M., and Ottesen, M. (1964) Isolation and properties of glutamine cyclotransferase of dried papaya latex, *Biochim. Biophys. Acta 92*, 409−411.
6. Fischer, W. H., and Spiess, J. (1987) Identification of a mammalian glutaminyl cyclase converting glutaminyl into pyroglutamyl peptides, *Proc. Natl. Acad. Sci. U.S.A. 84*, 3628−3632.
7. Schilling, S., Hoffmann, T., Manhart, S., Hoffmann, M., and Demuth, H.-U. (2004) Glutaminyl cyclases unfold glutamyl cyclase activity under mild acid conditions, *FEBS Lett. 563*, 191−196.
8. Saido, T. C., Iwatsubo, T., Mann, D. M., Shimada, H., Ihara, Y., and Kawashima, S. (1995) Dominant and differential deposition of distinct beta-amyloid peptide species, A beta N3(pE), in senile plaques, *Neuron 14*, 457−466.
9. Harigaya, Y., Saido, T. C., Eckman, C. B., Prada, C.-J., Shoji, M., and Younkin, S. G. (2000) Amyloid β protein starting pyroglutamate at position 3 is a major component of the amyloid deposits in the Alzheimer's disease brain, *Biochem. Biophys. Res. Commun. 276*, 422−427.
10. Ghiso, J., Revesz, T., Holton, J., Rostagno, A., Lashley, T., Houlden, H., Gibb, G., Anderton, B., Bek, T., Bojsen-Moller, M., Wood, N., Vidal, R., Braendgaard, H., Plant, G., and Frangione, B. (2001) Chromosome 13 dementia syndromes as models of neurodegeneration, *Amyloid 8*, 277−284.
11. Hashimoto, T., Wakabayashi, T., Watanabe, A., Kowa, H., Hosoda, R., Nakamura, A., Kanazawa, I., Arai, T., Takio, K., Mann, D. M., and Iwatsubo, T. (2002) CLAC: a novel Alzheimer amyloid plaque component derived from a transmembrane precursor, CLAC-P/collagen type XXV, *EMBO J. 21*, 1524−1534.
12. Sykes, P. A., Watson, S. J., Temple, J. S., and Bateman, R. C., Jr. (1999) Evidence for tissue-specific forms of glutaminyl cyclase, *FEBS Lett. 455*, 159−161.
13. Pohl, T., Zimmer, M., Mugele, K., and Spiess, J. (1991) Primary structure and functional expression of a glutaminyl cyclase, *Proc. Natl. Acad. Sci. U.S.A. 88*, 10059−10063.
14. Weisz, O. A. (2003) Acidification and protein traffic, *Int. Rev. Cytol. 226*, 259−319.
15. Bockers, T. M., Kreutz, M. R., and Pohl, T. (1995) Glutaminyl-cyclase expression in the bovine/porcine hypothalamus and pituitary, *J. Neuroendocrinol. 7*, 445−453.
16. Song, I., Chuang, C. Z., and Bateman, R. C., Jr. (1994) Molecular cloning, sequence analysis and expression of human pituitary glutaminyl cyclase, *J. Mol. Endocrinol. 13*, 77−86.
17. Schilling, S., Hoffmann, T., Rosche, F., Manhart, S., Wasternack, C., and Demuth, H.-U. (2002) Heterologous expression and characterization of human glutaminyl cyclase: evidence for a disulfide bond with importance for catalytic activity, *Biochemistry 41*, 10849−10857.
18. Schilling, S., Manhart, S., Hoffmann, T., Ludwig, H.-H., Wasternack, C., and Demuth, H.-U. (2003) Substrate specificity of glutaminyl cyclases from plants and animals, *Biol. Chem. 384*, 1583−1592.
19. Bateman, R. C., Temple, J. S., Misquitta, S. A., and Booth, R. E. (2001) Evidence for essential histidines in human pituitary glutaminyl cyclase, *Biochemistry 40*, 11246−11250.
20. Schilling, S., Niestroj, A. J., Rahfeld, J.-U., Hoffmann, T., Wermann, M., Zunkel, K., Wasternack, C., and Demuth, H.-U. (2003) Identification of human glutaminyl cyclase as a metalloenzyme: Inhibition by imidazole derivatives and heterocyclic chelators, *J. Biol. Chem. 278*, 49773−49779.
21. Booth, R. E., Lovell, S. C., Misquitta, S. A., and Bateman, R. C., Jr. (2004) Human glutaminyl cyclase and bacterial zinc aminopeptidase share a common fold and active site, *BMC Biol. 2*, 2.
22. Schilling, S., Hoffmann, T., Wermann, M., Heiser, U., Wasternack, C., and Demuth, H.-U. (2002) Continuous spectrometric assays for glutaminyl cyclase activity, *Anal. Biochem. 303*, 49−56.
23. Ellis, K. J., and Morrison, J. F. (1982) Buffers of constant ionic strength for studying pH-dependent processes, *Methods Enzymol. 87*, 405−426.
24. Fujiwara, K., and Tsuru, D. (1978) New chromogenic and fluorogenic substrates for pyrrolidonyl peptidase, *J. Biochem. 83*, 1145−1149.
25. Klockenkämper, R., and von Bohlen, A (2001) Total reflection X-ray fluorescence moving towards nanoanalysis: a survey, *Spectrochim. Acta B 56*, 2005−2018.
26. Huntington, K. M., Bienvenue, D. L., Wei, Y., Bennett, B., Holz, R. C., and Pei, D. (1999) Slow-binding inhibition of the aminopeptidase from *Aeromonas* proteolytica by peptide thiols: synthesis and spectroscopic characterization, *Biochemistry 38*, 15587−15596.
27. Dahl, S. W., Slaughter, C., Lauritzen, C., Bateman, R. C., Jr., Connerton, I., and Pedersen, J. (2000) Carica papaya glutamine cyclotransferase belongs to a novel plant enzyme subfamily: cloning and characterization of the recombinant enzyme, *Protein Expression Purif. 20*, 27−36.
28. Allary, M., Schrevel, J., and Florent, I. (2002) Properties, stage-dependent expression and localization of *Plasmodium falciparum* M1 family zinc-aminopeptidase, *Parasitology 125*, 1−10.
29. Auld, D. S. (1995) Removal and replacement of metal ions in metallopeptidases, *Methods Enzymol. 248*, 228−242.
30. Baker, J. O., and Prescott, J. M. (1983) *Aeromonas* aminopeptidase: pH dependence and a transition-state-analogue inhibitor, *Biochemistry 22*, 5322−5331.
31. Huang, K.-F., Liu, Y.-L., Cheng, W.-J., Ko, T.-P., and Wang, A. H.-J. (2005) Crystal structures of human glutaminyl cyclase, an enzyme responsible for protein N-terminal pyroglutamate formation, *Proc. Natl. Acad. Sci. U.S.A. 102*, 13117−13122.

BI051142E